

Block ramps for stream power attenuation in gravel-bed streams: a review

Rakesh Kumar Chaudhary, Nayan Sharma and Zulfequar Ahmad

ABSTRACT

Application of the block ramp technique in steep gradient streams for energy dissipation as well as to maintain river stability finds increasing favor amongst researchers and practitioners in river engineering. This paper dwells on a comprehensive state-of-the-art review of flow resistance, energy dissipation, flow characteristics, stability, and drag force on block ramps by various investigators in the past. The forms and equations for each type are thoroughly discussed with the objective of finding the grey areas and gaps. More research is warranted further to improve the equations, which are essential for design analysis. Block ramps can be a promising simple technique to achieve reasonable attenuation of devastating fluvial forces unleashed in gravel-bed streams during cloud bursts.

Key words | block ramp, drag force, energy dissipation flow resistance, stability

Rakesh Kumar Chaudhary (corresponding author)
Department of Water Resources Development and Management Indian Institute of Technology Roorkee,
Roorkee 247667,
India
E-mail: logtokumarakesh063@gmail.com

Nayan Sharma
Center for Transportation Systems (CTRANS), Indian Institute of Technology Roorkee,
Roorkee,
India

Zulfequar Ahmad
Department of Civil Engineering,
Indian Institute of Technology Roorkee,
Roorkee,
India

HIGHLIGHTS

- A critical review of recent advancement in flow resistance, energy dissipation, flow characteristics, stability and drag forces on block ramps.
- Highlights the grey areas and gaps.
- Need for 3D turbulent burst analysis for better understanding of the internal mechanism of turbulent structures.
- Application of all the equations in design with limitations and suggestions for improvement are well discussed.
- Formulation of block ramps is based on steady flow assumption but in reality flows are highly turbulent with unsteady flow in mountain streams.

INTRODUCTION

A block ramp is a short section of steep channel that produces large scale roughness in the form of a boulder, which allows passing flow from a higher elevation to lower elevation by dissipating energy (Aberle & Smart 2003; Pagliara & Chiavaccini 2006a; Ahmad *et al.* 2009). They are used in mountain rivers and are made of blocks with mean diameters ranging between 0.3 m and 1.5 m, disposed on a steep bed. Block ramps can serve very best in the

restoration of rivers and maintain the ecological balance of a river system as well as attenuate stream power.

Block ramps serve as corridors for fish migration by creating favorable flow velocity (Weibel & Peter 2013; Tamagni *et al.* 2014a, 2014b). They attenuate shear velocity and turbulent bursts adjacent to the bed, which prevents large boulder movement during flood. Moreover, protruding boulders also provide suitable conditions for oviposition.

Flow resistance, flow velocity and water depth can be estimated using flow resistance equations, which have been proposed by many investigators in terms of Manning's n and Darcy-Weisbach friction factor f (Hey 1979; Griffiths

This is an Open Access article distributed under the terms of the Creative Commons Attribution Licence (CC BY 4.0), which permits copying, adaptation and redistribution, provided the original work is properly cited (<http://creativecommons.org/licenses/by/4.0/>).

doi: 10.2166/ws.2020.339

1983; Jarret 1984; Bathurst 1985; Abt *et al.* 1988; Rice *et al.* 1988; Ferro 1999). Aberle & Smart (2003) studied the effect of roughness on flow resistance on steep slopes. They found that standard deviation of bed elevation is a more appropriate parameter for bed roughness than the characteristic grain size of the bed and used this parameter in a flow resistance equation. Similarly, Habibzadeh & Omid (2009) studied the bed load resistance in supercritical flow and found that bed load transport increases friction factors by 90% and 60% in smooth and rough beds respectively. Pagliara & Chiavaccini (2006a, 2006b, 2006c) proposed flow resistance and energy dissipation equations for block ramps.

Similarly, the stability of block ramps has been investigated by different investigators (Whittaker & Jäggi 1986; Robinson *et al.* 1995; Weichert 2006; Pagliara 2007a; Tamagni *et al.* 2008; Pagliara & Palermo 2011; Weitbrecht *et al.* 2017). Their findings are discussed in subsequent topics on the stability of block ramps. Studies on scour at the toe of the block ramp and its protection have been done by Pagliara & Hager 2004; Pagliara 2007b; Pagliara & Palermo 2006; Oertel & Schlenkhoff 2012b. They have developed empirical formula for estimation of maximum scour depth and maximum scour length for uniform and non-uniform sand. Moreover, they found that rock sill performed better than other types of sills for scour minimization. Besides this sediment transport over block ramp also has an effect on bed morphology and energy dissipation, which was later investigated by Pagliara *et al.* (2009a, 2009b).

Block ramps are very effective for dissipating energy downstream of trench weirs, overflow weirs, spillways and so on due to large roughness. Ghare *et al.* (2010) proposed a mathematical model for computation of the size of the base material of block ramps, which is correlated with the step chute height ratio. Similarly, Pagliara *et al.* (2019) found that equilibrium scour morphology is affected by channel bends, tail water depth and approach flow conditions. Increase in channel curvature increases scour depth and rise in tail water depth decreases scour depth. They also developed an empirical equation for estimation of maximum scour depth in a curve channel. Artur *et al.* (2018) measured the hydrodynamic parameters of a flood-impacted unstructured block ramp in prototype and found that boulders displaced due to flooding functioned as well as before the occurrence of the flood.

CLASSIFICATION OF BLOCK RAMP

Depending on the morphological structure and configuration of macro roughness elements, block ramps are classified into two groups; that is, type A (block carpet) and type B (block cluster). Type A consists of tightly packed blocks covering the entire width of the river. They may be in one layer or more than one layer. One layer of blocks interlocked with each other leading to a compact form is called an interlocked block ramp. When blocks are arranged in two or more than two layers leading to heavier and more heterogeneous construction then such block ramps are known as dumped blocks. With both types of block ramps, a filter layer should be provided against wash-out effects (DWA 2010). A block carpet can be provided up to slope $S = 10\%$ (Bezzola 2010). However, they are investigated up to bed slope $S = 40\%$ (Robinson *et al.* 1995). Type B are characterized by dispersed configuration leading to more natural conditions. In this group, blocks are either arranged in row and arches (systematic way) or randomly placed. Block ramps consist of three types of block ramps: structured blocks, unstructured blocks and self-structured blocks. Structured and unstructured blocks are isolated with each other. Structured blocks are characterized by systematic arrangements of blocks in rows or staggered and blocks are isolated from each other, leading to a more heterogeneous form. The maximum slope for a structured block ramp is 6.7% (LUBW 2006) and maximum slope for an unstructured block ramp (UBR) is 3% (Janisch 2007). Self-structured blocks ramps are formed due to natural hydraulic load occurring on the ramp over a long time. The ramp slope range for a self-structured block ramp is 5% to 13% (Lange 2007). The morphological and structural classification of block ramps is shown in Figure 1.

FLOW RESISTANCE

Knowledge of mean velocity is of primary importance in river engineering. Flow velocity can be directly measured by using a velocity-measuring instrument or using the continuity equation ($Q = UA$) for known discharge and cross-sectional area of flow. But velocity measurement is a tedious task and not always possible. So, there is a need for a flow

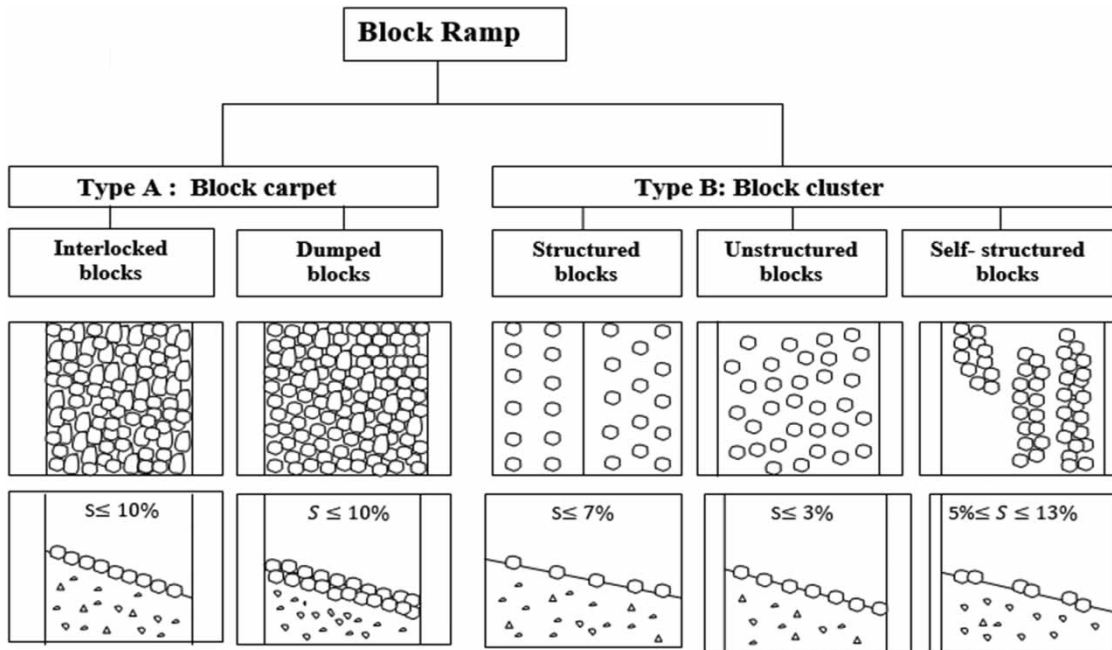


Figure 1 | Morphological and structural classification of block ramps (adapted after Tamagni et al. 2008).

resistance equation from which velocity can be determined by knowing other parameters such as flow depth, equivalent roughness height and so on. Flow resistance equations can be easily applied to any river reach of uniform section without calibration. The most commonly used flow resistance equations are the Chezy, the Manning's and the Darcy's Weisbach Equation and are as follows:

$$U = C\sqrt{RS} = \frac{1}{n}R^{2/3}S^{1/2} = \sqrt{\frac{8gRS}{f}} \quad (1)$$

where U = Mean flow velocity, Q = flow rate (L^3/S), C = Chezy coefficient ($L^{1/2}S^{-1}$), n = Manning's rugosity coefficient ($L^{-1/3}S$), f = dimensionless Darcy Weisbach friction factor, S = slope of energy grade line and R = hydraulic radius (for narrow channels) sometimes, depth of flow h is used for wide channels instead of R .

Several studies have been done to derive general equations for flow resistance in terms of Darcy Weisbach dimensionless friction factor f . Keulegan (1938) derived a general form of flow resistance equation for rough boundary channels by integrating the Prandtl-Karman-Nikuradse logarithmic mean velocity profile equation in the following

form:

$$\sqrt{\frac{8}{f}} = \frac{U}{u_*} = \frac{1}{k} \ln \frac{h}{k_s} + 6.25, \quad (2)$$

where u_* is shear velocity = \sqrt{ghS} , Keulegan (1938) proposed k_s by using it as equivalent to median diameter (D_{50}). Several expressions have been given for values of k_s such as $k_s = cD_x$ (where, $1 < c < 8$). Subscript x denotes the percentage finer of D . Weichert (2006) presented different definitions of k_s according to different studies. Bezzola (2010) suggested $k_s = 2d_{90}$ for flat natural river bed without bed forms. In boulder streams, the irregular bed topography makes it difficult to measure actual representative flow depth (h) and also D_{90} or k_s does not represent actual characteristic grain size. So, keeping this view, Aberle (2000) developed a flow resistance equation in terms of discharge and used σ_b as the standard deviation of bed elevation rather than flow depth (h) and D_{90} as characteristic grain size. The equation suggested by Aberle (2000) is as follows:

$$U = 0.81(\sin \alpha)^{0.18} q^{n_a} g^{0.5(1-n_a)} \sigma_b^{0.5(1-3n_a)}. \quad (3)$$

where $n_a = 0.87(\sin \alpha)^{0.09}$ and $\sin \alpha =$ bed slope, $q =$ specific discharge, $g =$ acceleration due to gravity.

Whatever approach is used to derive flow resistance equation, it is found that a flow resistance equation is more reliable on type of flow condition for which depth of flow or hydraulic radius is larger compared to bed roughness. Bathurst *et al.* (1981) defined roughness in three categories and proposed classifying flow according to relative flow depth. Large-scale roughness is ($h/D_{84} \leq 1.2$), in which a free surface is affected by roughness features, intermediate scale roughness ($1.2 < h/D_{84} \leq 4$), and small scale roughness ($h/D_{84} < 4$). They found that flow resistance increases as relative submergence decreases and vice versa. Various forms of expressions for relative submergence such as $h/d_{84}, h/d_{50}, h_{\text{mean}}/D_B$ and so on have been used in flow resistance equations by different investigators. It is difficult to model flow resistance for large and intermediate scale roughness since flow turbulence is strongly affected by relatively large roughness and hence Equation (2), derived from the law of wall, is not valid. It is valid for a steep mountain river with step pool morphology and flow on a block ramp is somewhat similar to it. Therefore, the above approach has to be applied with caution.

There is another approach for the determination of flow resistance for UBR in which flow resistance is divided into two parts. First part resistance is offered by the roughness of the bed material and second part is in the form of drag, developed due to the macro roughness element. Whittaker *et al.* (1988) used this approach to find flow resistance for UBR.

So, the flow resistance is given by the superposition of the two elements (Einstein & Banks 1950; Weichert 2007). With Chezy coefficients,

$$c' = \frac{U}{\sqrt{gRS'}} = 2.5 \ln \frac{12R}{K''} \quad (4)$$

This is the flow resistance due to the bed material; that is, bed roughness $S'' =$ slope of grain friction, $K' =$ equivalent sand roughness for the bed material; and

$$c'' = \frac{U}{\sqrt{gRS''}} = 2.5 \ln \frac{12R}{K''} \quad (5)$$

For the flow resistance due to macro roughness elements such as boulders, $S'' =$ slope of form friction,

$K'' = N_b D^3 (17.8 - 0.47 h/D) =$ equivalent sand roughness for macro roughness element; the flow resistance can be calculated with

$$\frac{1}{c^2} = \frac{1}{c'^2} + \frac{1}{c''^2} \quad (6)$$

Thus, both the block diameter D and number of blocks N_b is considered. The application range is limited to $0.1\% < S < 5\%$, $0.5 < h/d < 4$, and $N_b D^2 < 0.15$ per unit area. Whittaker *et al.* (1988) showed that submergence (h/D) has major influence on flow resistance.

In most studies, the influence of large scale roughness on flow resistance have been done but lacked the quantification of increase in flow resistance due to a large roughness element. So, Pagliara & Chiavaccini (2006c) did an experimental study on flow resistance of block ramps with protruding boulders placed in random and row arrangement. They combined friction factor f for rock chutes in base condition and increase in friction factor f_1 due to protruding boulders to get total friction factor and obtained following relation as:

$$\sqrt{\frac{8}{f_{\text{tot}}}} = \frac{U}{\sqrt{ghS}} = 3.5(1 + \Gamma)^c S^{-0.17} (h/d_{84})^{0.1} \quad (7)$$

$$\text{or, } \sqrt{\frac{8}{f_{\text{tot}}}} = \frac{C}{\sqrt{g}} = 3.5(1 + \Gamma)^c S^{-0.17} (h/d_{84})^{0.1}$$

where, $U = C\sqrt{hS}$, (Chezy's equation) also the total Manning's coefficient n_{tot} ,

$$n_{\text{tot}} = 0.064(1 + \Gamma)e \times (d_{50}S)^{0.11} \quad (8)$$

where, block concentration $\Gamma = \frac{N_B \pi D^2}{4WL}$, in which, $N_B =$ number of blocks, $D =$ block diameter = ramp width and $L =$ ramp length. Valid for range $0.8 < F < 2.9$, $0 < \Gamma < 0.3$ and $0.6 < h/d_{84} < 2.6$. where F and h/d_{84} are the Froude number and submergence ratio, respectively. c and e are coefficients derived from experimental measurements and observed data, whose values are listed in Table 2. Equation (7) obtained by Pagliara & Chiavaccini (2006c) for flow resistance estimation of block ramps with protruding boulders, considers the effect of slope as well as a new term, boulder concentration Γ . This equation shows that the Chezy coefficient can be expressed as a decreasing monotonic function

of the boulder concentration. Thus is in contrast with findings of other authors (Rouse 1965; Wohl & Ikeda 1998). According to Wohl & Ikeda (1998) study, it is reasonable that the Chezy coefficient decreases with boulder concentration up to a certain range and then increases with boulder concentration for given geometrical and hydraulic conditions. Hence, Equation (7) is not valid for larger values of block concentration ($\Gamma > 30\% - 35\%$). Figure 2(b) depicts the range of validity and variation of the Chezy coefficient, C , with block concentration Γ . It follows previous research findings and is valid up to a range $\Gamma = 0.3$.

Equation (7) proposed by Pagliara & Chiavaccini (2006c) used d_{84} of bed material in relative submergence (h/d_{84}) instead of considering protruding boulder mean diameter. The protruding boulders create additional resistance to flow. So, it overestimates mean flow velocity on the block ramp. Later on Weitbrecht et al. (2017) considered protruding boulder protrusion P in Equation (7) and finally, they proposed the following relation.

$$\sqrt{\frac{8}{f_{tot}}} = \frac{U}{\sqrt{ghS}} = 1.9(1 + \Gamma)^{-0.5} S^{-0.21} (h/P)^{0.29} \quad (9)$$

Valid for $h/p < 3.5$, $0.15 < \Gamma < 0.25$.

The flow resistance Equation (9) is valid for a minimal range of block concentration, so it is necessary to find out

a more generalized form of flow resistance equation that covers a larger range of block concentration. Several studies on finding the optimal value of block concentration Γ have been done to achieve maximum flow resistance (Schlichting 1936; Loughlin & MacDonald 1964). Thus, one can determine flow resistance, flow velocities and flow depth using one of the standard flow resistance equations discussed above and in Table 1.

Some of the widely used flow resistance equations for block ramp is briefly presented in Table 1 with their application range.

ENERGY DISSIPATION ON BLOCK RAMPS

The energy head at the ramp head is $H_1 = H + 1.5 h_c$, where $1.5 h_c$ is the specific energy at a critical depth (at the head of a ramp), and at the toe is $H_2 = h + q^2/(2gh^2)$, specific energy at toe. So, the relative energy dissipation is given as $\Delta H_r = \Delta H/H_0 = \frac{H_1 - H_2}{H_1}$. Pagliara & Chiavaccini (2006a) studied the energy dissipation mechanism on smooth ramps and ramps with a base material. They first studied a smooth ramp and then an on-ramp with blocks.

A smooth ramp is highly representative as a chute in terms of hydraulic characteristics of flow. Chanson (1994) suggested the energy dissipation relation between inlet and

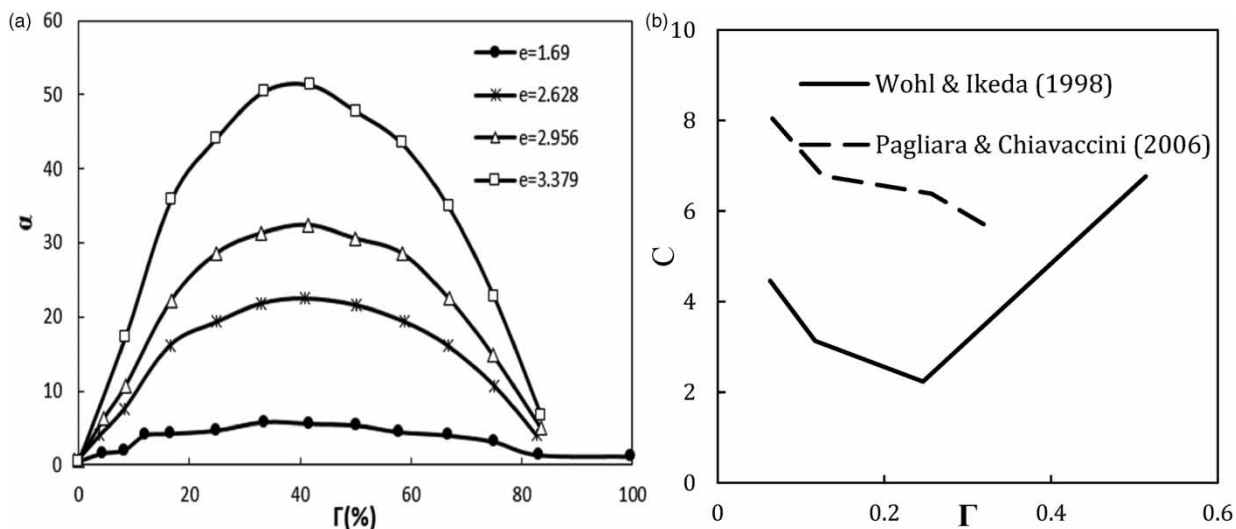


Figure 2 | (a) Relationship between Γ and α for given e ($=D_{50}/d_{50}$) values (Ferro 1999) and (b) Chezy coefficient C as a function of macroroughness concentration Γ for a transverse row disposition of macroroughness.

Table 1 | Flow resistance equation proposed by various investigators

Investigator	Relation/Equation	Description
Scheuerlein (1968)	$\sqrt{\frac{8}{f}} = \frac{U}{u_*} = 3.93 \ln\left(\frac{h}{\eta(0.425 + 2.025S)K}\right)$ (10)	For block ramp of type A with interlocked block, $\eta < 1 =$ air content parameter, $\Phi = DN^{1/2} =$ packing factor, $D =$ equivalent block diameter, $K = D/3 =$ mean roughness height, applicable for bed slope $10\% < S < 67\%$
Rice et al. (1988)	$\sqrt{\frac{8}{f}} = \frac{U}{\sqrt{ghS}} = 2.21 \ln(h/d_{84}) + 6.00$ (11)	It is applicable for block ramps of type A with dumped blocks. Valid for bed slope $2.8\% < S < 33\%$ and median rock diameter $52 \leq D_{50} \leq 278$ (mm)
Ferro (1999)	$\sqrt{\frac{8}{f}} = 15.74 \log \frac{h}{d_{84}}$ (12)	$b_o = -1.5$ for $\Gamma > 50\%$, $b_o = -(0.2590 - 0.1189\alpha - 0.01711\alpha^2 + 0.00117\alpha^3)$ for $\Gamma > 50\%$ and α for various $e = D_{50}/d_{50}$ from Figure 2
Aberle & Smart (2003)	$\sqrt{\frac{8}{f}} = 3.54 \ln \frac{h}{d_{84}} + 4.41$ (13)	Derived with experimental data with $d_{90} = 64$ mm and $d_{10} = 32$ mm randomly placed at $S = 8\%$ to 10%
Oertel & Schlenkhoff (2012a, 2012b)	$\sqrt{\frac{8}{f}} = \left(4.4 + \frac{0.09}{S}\right) \log \frac{h}{D_B} + \left(2.2 + \frac{0.0023}{S}\right)$ (14)	Derived for crossbar block ramps with boulder height of crossbars as D_B . It is valid for relative submergences $1.5 < h/D_B < 4$ and for tested ramp slopes $2\% < S < 10\%$

Table 2 | Values of the coefficient of c and e

Coefficient	Random arrangement, rounded aggregate	Row arrangement rounded aggregate	Random arrangement, crushed aggregate	Row arrangement crushed aggregate
c	-1.60	-1.80	-2.40	-3.00
e	1.00	1.20	1.80	2.30

the toe of a smooth ramp chute as:

$$\Delta H_r = 1 - \left(\frac{h_u \cos\theta + h_c}{1.5h_c + H}\right) \tag{15}$$

where ΔH_r is relative energy dissipation, $h_u =$ uniform flow depth at toe of ramp and $h_c =$ critical flow depth at the inlet, as shown in Figure 3. Pagliara & Chiavaccini (2006a) suggested a relationship for smooth ramps and ramps with base material as blocks in terms of Darcy-Weisbach friction factor f .

$$\Delta H_r = \frac{\Delta H}{H_1} = 1 - \frac{\left[\left(\frac{f}{8S}\right)^{1/3} \cos \alpha + \frac{1}{2} \left(\frac{f}{8S}\right)^{-2/3}\right] \frac{h_c}{H}}{1.5 \frac{h_c}{H} + 1} \tag{16}$$

They found that the form of Equation (16), however, doesn't fit the experimental data well, especially for

smooth ramps, and finally, they suggested the following relationship.

$$\Delta H_r = \frac{\Delta H}{H_1} = \frac{H_1 - H_2}{H_1} = [A + (1 - A)e^{(B+CS)(h_c/H)}] \tag{17}$$

A, B, C = coefficients depending on the roughness scale (h_c/d_{50}) and E, F = function of arrangement and roughness of blocks $h_c =$ critical flow depth $d_{50} =$ median size of river bed material, $H =$ ramp height and $S =$ ramp slope.

Pagliara & Chiavaccini (2006a) found that the relative energy dissipation (ΔH_r) increases with decrease in h_c/H for the same discharge, same slope and same length of ramp. thus, the height of the ramp is directly proportional to the relative energy dissipation. Similarly, the roughness of the bed also has a significant effect on relative energy dissipation. Large-scale roughness (LR) dissipates more energy than small-scale roughness (SR) whereas intermediate scale roughness (IR) presents greater variability. As is

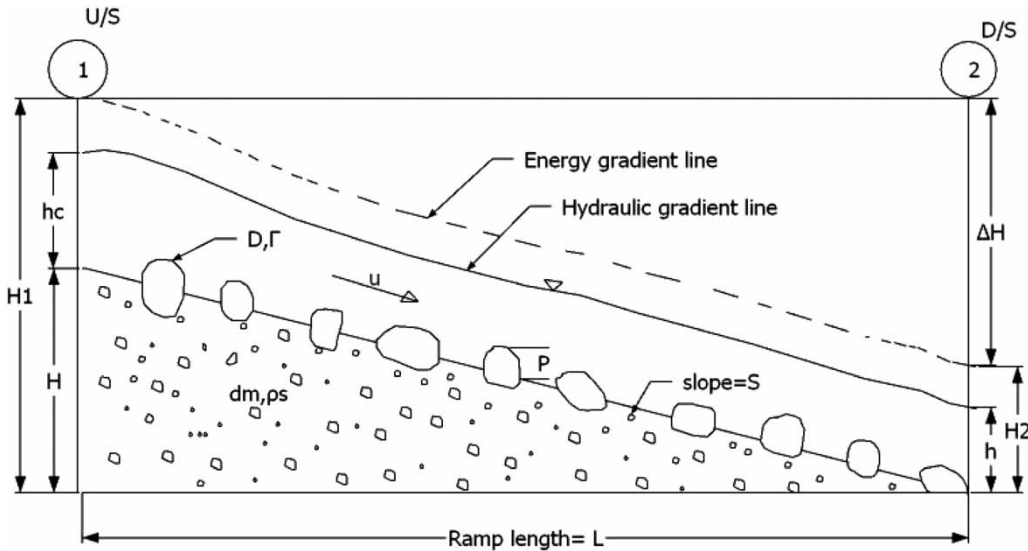


Figure 3 | Definition sketch of UBR for determination of energy dissipation (Tamagni 2013).

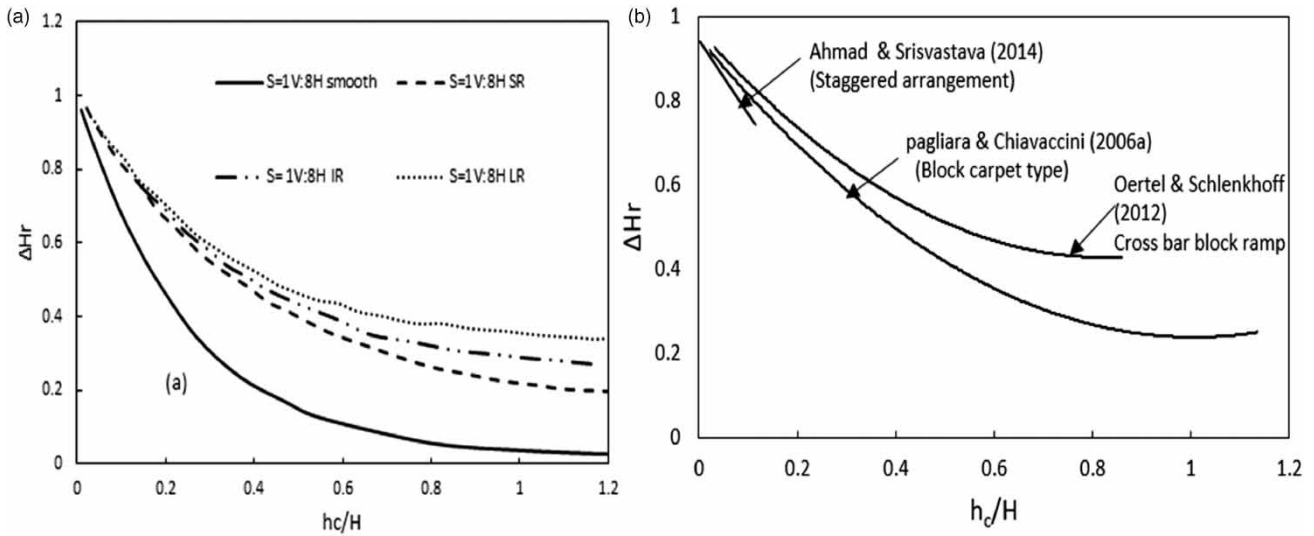


Figure 4 | (a) Relative energy dissipation for different ramp slopes and different roughness scales by Pagliara & Chiavaccini (2006a) and (b) by different investigators.

shown in Figure 4(a), they also found that relative energy dissipation decreases with an increase in slope, keeping roughness constant. So, energy dissipation is also a function of the slope of the ramp. Figure 4(b) shows relative energy dissipation as a function of h_c/H obtained by various investigators.

Pagliara & Chiavaccini (2006b) extended the energy dissipation mechanism to structured and unstructured block ramps, and proposed a relation, the same as Equation

(17), in which block concentration Γ was introduced.

$$\Delta H_{rb} = \frac{\Delta H}{H_1} = \frac{H_1 - H_2}{H_1} = [A + (1 - A)e^{(B+CS)(hc/H)}] \left(1 + \frac{\Gamma}{E + F\Gamma} \right) \quad (18)$$

$\Gamma = \frac{N_B \pi D^2}{4WL}$, where, N_B = number of blocks, D = block diameter, W = ramp width and L = ramp length. It can be used for ramps without boulders by substituting $\Gamma = 0$.

Here, E and F are two parameters that are functions of arrangement and roughness of blocks, which are given in Tables 3 and 4. Equation (18) is valid for $\Gamma < 0.33$; $0.08 < S < 0.33$; $1.75 < D/d_{50} < 19$ and for uniform flow conditions.

Figure 5 depicts that arrangement of boulders in rows dissipates more energy than random arrangement and this is higher for rough boulders than smooth (rounded) boulders. Rouse (1965) suggested optimum block concentration $\Gamma = 0.26$ using spheres. But for lower values of Γ , the maximum value of relative roughness and form drag are not get achieved and whereas a higher value of Γ leads to effects on flow characteristics by single blocks to other neighbouring blocks, flow separation cannot develop fully leading to reduced energy dissipation. Thus, at optimum value of block concentration Γ , each block offers maximum form drag to flow resistance.

Later on, Ahmad et al. (2009) found that the energy dissipation in a staggered arrangement of boulders on a ramp is higher than for a random or row arrangement of boulders. They proposed a relationship based on extensive experimentation on a staggered arrangement of hemispherical boulders on ramp. These values were validated with the experimental observations of authors within $\pm 3\%$ error line. Adopting the roughness parameter $E = 0.6$ and $F =$

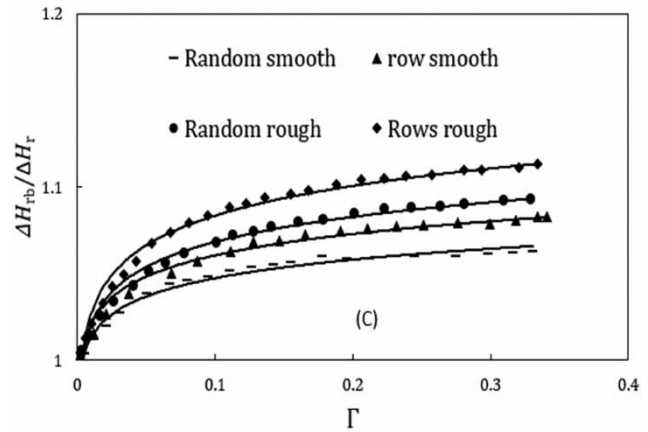


Figure 5 | Shows increase in relative energy dissipation according to Equation (18) for rounded (smooth) and crushed (rough) blocks for different block concentration Γ (Pagliara & Chivaccini 2006b).

$7.9 \left(\frac{D_B}{h_c}\right)^{-0.9}$, keeping the original form of the equation same as suggested by Pagliara & Chivaccini (2006b)

$$\frac{\Delta H}{H_1} = \frac{H_1 - H_2}{H_1} = \left[A + (1 - A)e^{(B+CS)(hc/H)} \right] \times \left(1 + \frac{\Gamma}{0.6 + 7.9 \left(\frac{D_B}{h_c}\right)^{-0.9} \Gamma} \right) \quad (19)$$

Table 3 | Values of A, B, and C for different roughness condition and ranges of h_c/d_{50}

Roughness condition	h_c/d_{50}	A	B	C
Large scale roughness	$h_c/d_{50} < 2.5$	0.33	-1.3	-14.5
Intermediate scale roughness	$2.5 < h_c/d_{50} < 6.6$	0.25	-1.2	-12.0
Small scale roughness	$6.6 < h_c/d_{50} < 42$	0.15	-1.0	-11.5
smooth ramp	$h_c/d_{50} > 42$	0.02	-0.9	-25.0

Table 4 | Values of E and F for different arrangement and roughness of boulder

Arrangement and roughness of boulder	E	F
Random disposition and rounded boulders (River stones)	0.6	13.3
Row disposition and rounded boulders	0.55	10.5
Random disposition and crushed boulder (Quarry stones)	0.55	9.1
Row disposition and crushed boulder	0.4	7.7

In this Equation, Γ varies from 0.074 to 0.21 and D_B/h_c from 0.506 to 2.307

Though Equation (19), proposed by Ahmad et al. (2009), is the outcome of a staggered arrangement of hemispherical boulders on a ramp, but in nature, we mostly find irregular shapes of boulder. So, further research can be extended on block ramps with irregular natural shapes of boulders in a staggered arrangement.

Similarly, Oertel & Schlenkhoff (2012a, 2012b) proposed Equation (20) for energy dissipation for a structured block ramp with crossbar as:

$$\frac{\Delta H}{H_1} = \frac{H_1 - H_2}{H_1} = a_1 + (1 - a_1)e^{\left[\frac{(a_2+a_3S)h_c}{H} \right]} \quad (20)$$

where, $a_1 = 0.17 - 0.0017/S$, $a_2 = -0.7 + 0.0073/S$, $a_3 = -4.9 - 0.26/S$. Equation (20) is valid for tested data range as of Equation (14).

Later on, Romeji *et al.* (2020) developed a generalized equation for energy dissipation for uniform and non uniform staggered arrangements of boulder block ramps based on experimental work, as given by Equation (21).

$$\Delta E_r = L_R a_1 e^{\left[\frac{a_2}{a_3 + \Gamma \left(\frac{h_c}{H} \right)} \right]} \quad (21)$$

where, L_R is length of ramp, a_1 , a_2 , a_3 are coefficients whose values are given in Table 5 and the rest are the same as discussed above. The above equation is applicable for $\Gamma = 0.17-0.30$ and $0.05 < h_c/H < 0.29$.

For submerged flow conditions, Pagliara *et al.* (2008) developed an equation for energy dissipation on submerged block ramps and identified the main parameters on which energy dissipation on block ramps in submerged condition depend.

These are h_c/H , ramp scale roughness and the ramp submergence condition. The effect of ramp slope can be

considered negligible for relative energy dissipation for the same scale roughness and ramp submergence conditions (L_j/L_R), as shown in Figure 6.

$$\Delta H r_2 = A + (1 - A)e^{(B)h_c/H} \quad (22)$$

This is valid for range: $0 < L_j/L_R < 0.7$, $0.1 < h_c/H < 1.2$; ramp slope varying between 1 V:8H and 1 V:4H and roughness condition SR, IR and LR. The expression of coefficients A and B are given in Table 6.

The equation proposed by Pagliara *et al.* (2008) for block ramps in submerged flow condition considers h_c/H as the main parameters in the energy dissipation equation, but when the flow is fully submerged the parameters h_c/H do not clearly reflect the hydrodynamics of submerged flow. Instead of the h_c/H term, it would be better to use h/d_{84} or h/P . So, further research is needed for improvement of the energy dissipation equation in submerged flow conditions.

The details of the experimental setup and parameters used by various investigators in the past have been summarized in Table 7.

Table 5 | Values of coefficient a_1, a_2 and a_3 for different values of Γ

Γ	a_1	a_2	a_3
0.17–0.19	0.110	0.053	0.064
0.20–0.21	0.020	0.834	0.332
0.22–0.24	0.051	0.323	0.207
0.25–0.26	0.074	0.173	0.140
0.27–0.30	0.012	1.616	0.530

FLOW CHARACTERISTICS

The block ramp offers high resistance as a result of form drag, wake vortices, local hydraulic jump, and jetting flow between each block. Flow over a block ramp or rock

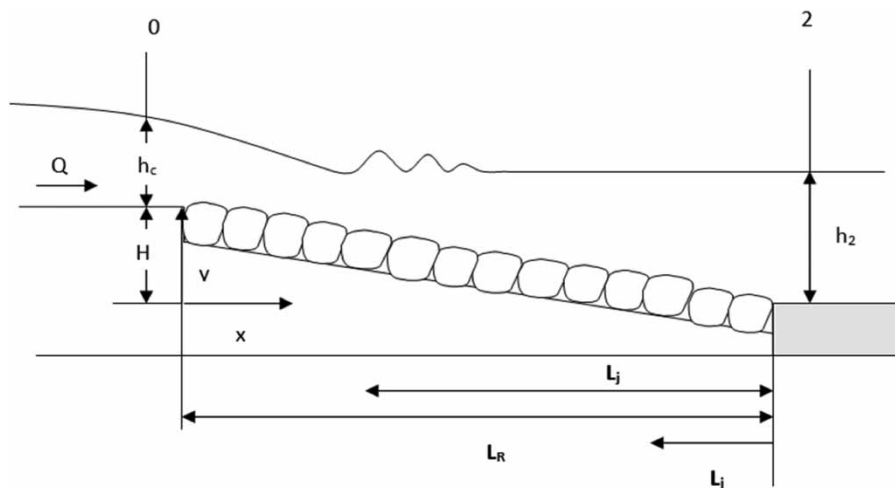


Figure 6 | Definition sketch of submerged block ramp (Pagliara *et al.* 2008).

Table 6 | Expression of coefficients of A and B for Equation (22) for different roughness conditions

Roughness condition	A	B
SR	$0.0239e^{-2.325(L_j/L_R)}$	$-(10.7 L_j/L_R + 1.729)$
IR	$0.0249e^{-1.618(L_j/L_R)}$	$-(9.95 L_j/L_R + 1.863)$
LR	$0.256e^{-1.245(L_j/L_R)}$	$-(8.475 L_j/L_R + 1.931)$

chutes shows two types of flow, such as nappe flow and skimming flow. Nappe flow occurs for small discharges. In this, flow cascades over a boulder in a series of falls, plunges from one boulder to another boulder in a thin layer that clings to the surface of each boulder, and dissipates the energy of flowing water by breaking a jet in the air or a jet impinging on a boulder, mixing of flow, and by partial hydraulic jump. Skimming flow occurs at high discharges. In skimming flow, the water flows down the boulder surface as a coherent stream, skimming over the boulder edge and cushioned by the recirculating fluid trapped between them.

Ahmad *et al.* (2013) investigated the turbulence characteristics of flow over a block carpet-type block ramp. The findings from their research are as follows.

Turbulent intensity and Reynolds stress distribution: longitudinal turbulence intensity TI_u increases first and then becomes constant after a certain distance. At the leading edge of the block ramp, the boundary layer was thin, and the generated turbulence intensity was confined in it. This is due to the fact that initially, the thickness of the boundary layer was thin, and then it increased downstream and became constant up to flow depth. So, turbulence intensity also increases downstream of the block ramp and becomes constant (Ahmad *et al.* 2013). Similar results were also obtained by Balachandar & Patel (2002), who studied development of a boundary layer on a roughened flat plate. However, transverse turbulence intensity decreases and then attains a constant value after a certain distance downstream of the block ramp, and vertical turbulence intensity TI_w decreases gradually downstream, as shown in Figure 7(a). This might be due to the breaking of larger eddies into smaller eddies, which dampens the turbulence intensity TI_v production.

Similarly, Ahmad *et al.* (2013) found that Reynolds stress components $\overline{u'v'}$ and $\overline{u'w'}$ increase first and then attain an equilibrium value, whereas $\overline{v'w'}$ increases linearly along the block ramp, which Figure 7(b) depicts clearly. Also,

turbulent kinetic energy increases linearly along the length of the block ramp.

Flow characteristics of an unstructured or structured block ramp are far more complex than other types. For this, Tamagni *et al.* (2014a, 2014b) carried out extensive experimentation on flow characteristics of unstructured block ramps under steady conditions for three different specific discharges with relative submergence such that $h < p$ (where p is block protrusion); that is, blocks emerged, $h \approx p$; that is, blocks just submerged and $h > p$; that is, blocks fully submerged. They divided flow into different sublayers as suggested by Nikora *et al.* (2001), as is shown in Figure 8. Here, they divided flow layers into two major sub layers for small value of submergence $h/p < 1.5$ and impermeable bed layer. They are a form induced sublayer and interfacial sublayer. The interfacial sublayer further consists of two sublayers where flow is affected by macroroughness elements and a lower sedimentary sublayer. All layers' thicknesses are denoted by z with different subscripts. Here, z_m is the mean bed level obtained by averaging the measured bed elevations without considering block protrusions, σ_b is the standard deviation of measured bed elevations, $2\sigma_b$ is the thickness of the sedimentary sublayer, z_z , the zero plane defined as $z_z = z_m - \sigma_b$ and Z_{MR} , the boundary between the macroroughness sublayer and sedimentary sublayer $Z_{MR} = z_m + \sigma_b$. Similarly, z_c is the average of the crest height of all blocks, from which we get the thickness of the macro roughness sublayer and z_t , defined as the lowest trough level of the bed.

The data were analyzed both with time-averaged and double averaged (in time and space) velocities, using measured Reynolds stress, form induced stress, and RMS values. From their study, they found that there exists a wide range of regions of varying velocities, which is favorable for fish migration. On just the lee side of the block, time average local velocity is negative due to recirculation of flow. Similarly, just upstream and above the block, there is a supercritical flow region having accelerated flow and also a small velocity range because the accelerated overtopping flow does not occur over each block for $h_m/p = 0.6$. It also shows that flow velocity between two blocks along the ramp length is positive unless it gets restarted by downstream blocks. In this way there exists strong heterogeneous distributions of a wide range of local velocities. The larger the variation in local velocities, the greater will be

Table 7 | A brief summary of the experimental setup and range of parameters used by various investigators

Author	Type of block ramp	Flume dimension(m)			Slope(s)	Block dia (mm)	Base material d ₅₀ (mm)	F	σ, C _u	Q (m ³ /s)
		Length	Width	Depth						
Pagliara & Chiavaccini (2006a)	Interlocked blocks(Type A)	3.5	0.25	0.3	1 V:4H-	1.0	1.4–4.3	1.2–1.5 (C _u)	0.001–0.025for Flume 1,2 0.006–0.1 for flume 3
		6.0	0.35	0.5	1 V:12H		2.0			
		25	0.8	0.9	1 V: 8H		10.0 20.0 88.0			
Pagliara & Chiavaccini (2006b)	Reinforced block ramp	3.5	0.25,	0.3	0.08–0.33	29, 38, 42	2, 3.5, 12.3, 16.5, 21.7	0.95–3.9
Pagliara <i>et al.</i> (2008)	Submerged block ramp	3.5	0.25	0.3	1 V:4H- 1 V: 8H	1.0 2.0 10.0 20.0	1.1–1.3 (C _u)	0.002–0.008
Ahmad <i>et al.</i> (2009)	Block ramp with staggered boulder	4.12	0.3	1 V:4H	55, 65, 100	20	0.077–0.0297
Oertel & Schlenkhoff (2012a, 2012b)	Cross bar block ramp	6	0.8	1 V:30H	60	2	0.001–0.05
Tamagni <i>et al.</i> (2014b)	Unstructured block ramp	8	0.4	0.7	0.04	65	4.3	3.2 (σ)	0.07
Weitbrecht <i>et al.</i> (2017)	Unstructured block ramp	13.5	0.6	0.6	0.05	43, 57, 65	1.5 (FM) 3.1(UM-FM) 4.3 (CM) 8.5(UM-CM)	1.1–3.3 (σ)	0.00018–0.084
Romeji <i>et al.</i> (2020)	Uniform and non uniform staggered boulder	4.0	0.3	0.45	1 V:5H 1 V:7H 1 V:9H	42–100	16–25	0.0073–0.0387

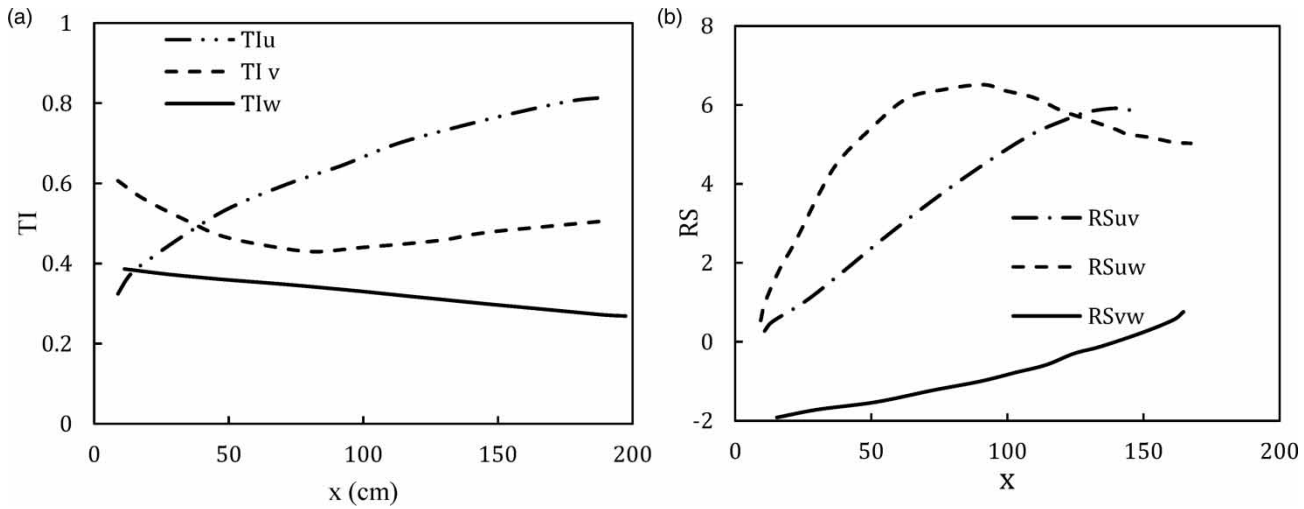


Figure 7 | (a) Variations of longitudinal u' , transverse v' and vertical w' turbulence intensity along length of ramp (Ahmad et al. 2013). (b) Variation of Reynold's Stress along length of block ramp (Ahmad et al. 2013).

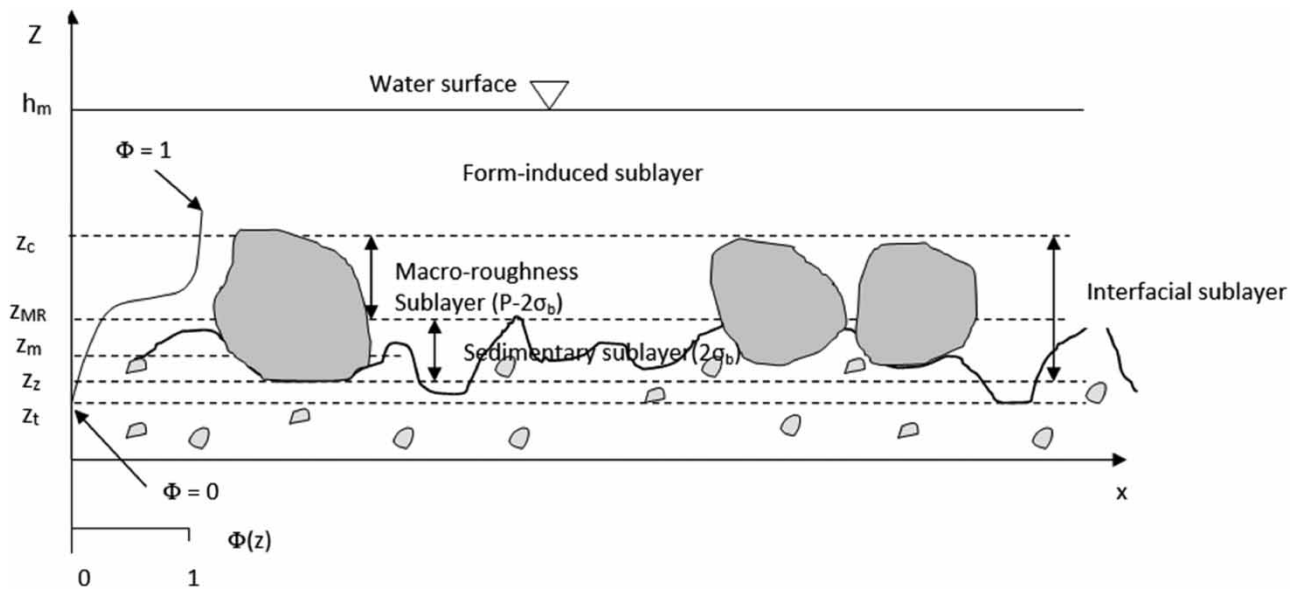


Figure 8 | Proposed flow sub-divisions suggested by Tamagni et al. (2014a, 2014b) for lower submergence ratio and impermeable bed layer based on guidelines of Nikora et al. (2001).

possibilities of certain fish to find suitable conditions for migration of fish with respect to swimming capacity.

Over all, the local time-averaged velocities are heterogeneously distributed on an unstructured block ramp, which leads to vary turbulence intensities heterogeneously. Zones that have high TI corresponds to two kinds of regions.

(i) The regions having high-velocity variation are directly influenced by blocks and recirculation of flow occurs in the lee side of protruding boulders.

(ii) Those adjacent to the flow corridor have accelerated velocity.

So, there is variability in both turbulence intensity as well as time averaged velocity, which is positive in terms of hydraulic heterogeneity and ecological aspects.

Though the time-averaged velocities were found to be heterogeneously distributed throughout the length of the ramp, the double averaged (averaged both in time and space) velocity \bar{u} profile is found to be almost uniform distribution as shown in Figure 9.

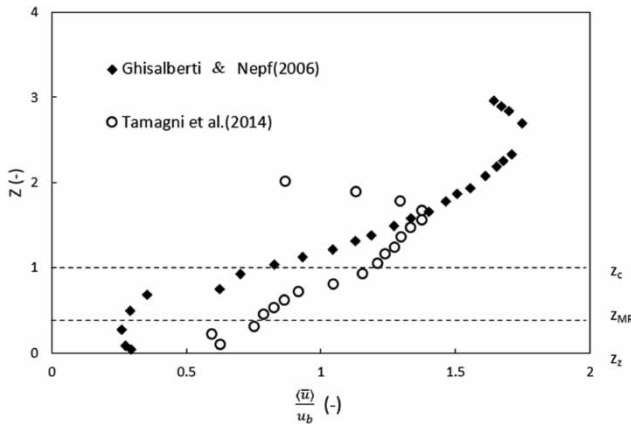


Figure 9 | Vertical distribution of normalized velocities $\langle \bar{u} \rangle / u_b$ by Tamagni et al. (2014a, 2014b) and Ghisalberti & Nepf (2006) for $h_m/p = 1.5$. where u_b is the bulk velocity.

For lower relative submergence, flow mainly occurs below the boulder crest, where the flow is influenced by form drag within the interfacial sublayer (macro roughness layer). Similarly, near the bed, level flow is dominated by form and viscous drag (sedimentary sublayer). The entire water column is affected by total roughness of the bed material and boulder and for this reason double averaged vertical velocity profile is uniform at higher relative submergence $h_m/p = 1.5$, it strongly varies and tends to an S-shape velocity profile similar to Bathurst (1985); Ferro (1999) and Baiamonte & Ferro (1997). Tamagni et al. (2014b) compared S-shape vertical velocity profile distribution results with those of Ghisalberti & Nepf (2006), which are similar to their results, as shown in Figure 9.

Similarly, they calculated normalized spatially averaged Reynolds shear stress, given as $\frac{-\overline{u'w'}}{u_{*I}}$, where $u_{*I} = (-\overline{u'w'}_{\max})^{0.5}$ in which u' , w' are fluctuating components of instantaneous velocity u , w . Figure 10 shows comparison of the vertical profile of spatially averaged Reynolds shear stress by Tamagni et al. (2014a, 2014b) and Ghisalberti & Nepf (2006) for $h_m/p = 1.5$, which has a triangular shape with its maximum value at $Z \approx 0.83$ just below z_c , at which the maximum momentum exchange occurs due to the maximum interaction between fluid at the form-induced sublayer and the macro roughness sublayer. The shape of both profiles is similar. Similarly, study on flow characteristics of a staggered arrangement of boulders on a rock ramp fish pass in relation to fish passage was done by Baki et al. (2014).

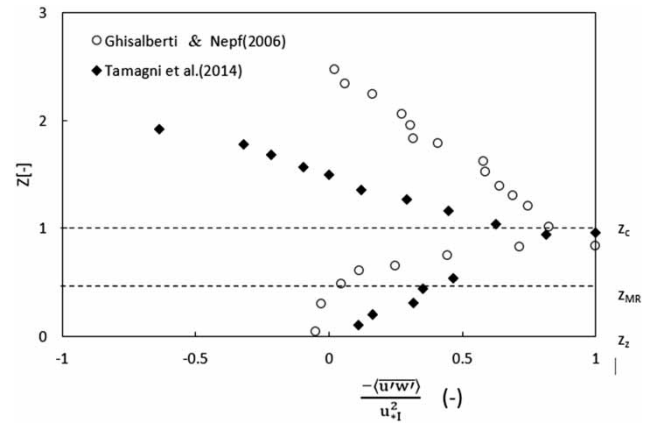


Figure 10 | Vertical distribution of normalized spatially averaged Reynolds shear stress $\frac{-\langle \overline{u'w'} \rangle}{u_{*I}^2}$ by Tamagni et al. (2014a, 2014b) and Ghisalberti & Nepf (2006) for $h_m/p = 1.5$.

BLOCK RAMP STABILITY

Stability is another important aspect of the block ramp for its proper functionality. It must withstand design flood discharge. Thus, it is important to estimate discharge at which the block just fails and such discharge is known as critical discharge, usually expressed as critical specific discharge q_{cr} . A block resting on the river bed remains stable unless shear stress imposed by flowing water exceeds the tractive shear stress of the block. So, a critical flow parameter must be known. Generally, Shields (1936) method is used to estimate critical flow parameters; that is, Shields dimensionless critical shear stress and dimensionless Reynolds number. But the Shields approach is valid for a nearly horizontal bed in which the component of gravity can be neglected. Chiew & Parker (1994) proposed a relationship for estimation of critical shear stress in a streamwise bed slope by considering all the hydrodynamic forces (drag, lift, buoyant and gravity force) acting on sediment particles resting on the streamwise bed slope given by:

$$\frac{\tau_{c\theta}}{\tau_{co}} = \cos \theta \left(1 + \frac{\tan \theta}{\tan \phi} \right) \quad (23)$$

where, $\tau_{c\theta}$ is the critical shear stress on the sloping bed of angle θ , τ_{co} = critical shear stress on the horizontal bed and ϕ is the friction angle of the sediment. However, mountain streams are characterized by a low value of relative

submergence and steep bed slope of large-scale roughness. So, the Shields approach is not suitable for mountain streams. Later on, Aguirre-Pe & Fuentes (1991) put forth their concept that critical shear stress doesn't represent the condition for initiation of sediment motion in steep macroroughness streams ($S \geq 0.005$ and $h/d \leq 10$). Aguirre-Pe *et al.* (2003) suggested a relationship for sediment entrainment in terms of critical particle densimetric Froude number given as:

$$F_{dc} = 0.9 + 0.5 \ln \frac{h}{d_{50}} + 1.3 \frac{d_{50}}{h} \quad (24)$$

which is valid for $0.02 < S < 0.065$; $0.02 < h/d_{50} < 30$.

But for field engineers, it would be worth expressing failure criteria in terms of critical specific design discharge rather than critical particle densimetric Froude number.

Whittaker & Jäggi (1986) investigated the stability of a block carpet type block ramp with different block diameters, bed materials, characteristic grain sizes, bed slopes and different ramp lengths.

They suggested a relationship between critical specific discharge q_{cr} , bed slope S and block diameter D_{65} for the determination of stability of block ramps of block carpet (type A) with dumped blocks.

$$q_{cr} = \frac{0.257}{S^{7/6}} \sqrt{g(G-1)D_{65}^3} \quad (25)$$

where S = bed slope, G = specific gravity of block = $\frac{\rho_s}{\rho_w} = 2.65$ and D_{65} = block diameter for which 65% of the mixture is finer, ρ_s is density of block and ρ_w is density of water.

Hartung & Scheuerlein (1970) suggested a relationship for block ramp type A with interlocked blocks in terms of critical velocity u_{cr} :

$$u_{cr} = 1.2 \sqrt{2g(G-1)D_B \cos \alpha} \quad (26)$$

where u_{cr} = critical flow velocity, D_B = equivalent block

diameter and other terms are as defined above.

$$D_B = \sqrt[3]{\frac{6m_B}{\pi\rho_s}} \quad (27)$$

where m_B = mass of block, $D_B = 1.06 D_{65}$

Robinson *et al.* (1995) investigated the stability of rock chutes for slopes ranging from 0.1 to 0.4 and suggested a relationship for estimation of critical specific discharge q_{cr} at failure of blocks as:

$$q_{cr} = (D_{50}S)^{(1.40+0.213/\sqrt{S})} \exp(-11.2 + 1.46/\sqrt{S}) \quad (28)$$

where D_{50} = is the median size of blocks, S = slope of ramp. In this experiment, the investigated chutes were made of layers of thickness $2D_{50}$ placed over geotextile as a filter medium.

According to Aberle (2000) the stability of block cluster type is determined with:

$$q_{cr} = 0.062S - 1.11 \sqrt{g(G-1)D_B^3} \quad (29)$$

This has the same structure as Equation (25) but has a lower value of numerical coefficient and slightly lower power coefficient of the ramp slope S .

Pagliara & Chiavaccini (2007) investigated three boulder configurations (blocks in rows, random and arc configuration) and proposed a relationship for estimation of critical specific discharge

$$\frac{q_c}{q_{co}} = (1 + 0.084\Gamma)^{2.7} \quad (30)$$

where q_c is critical failure discharge of reinforced chutes and q_{co} is one for base chutes and Γ is block concentration as discussed above.

Pagliara & Chiavaccini (2007) extended the investigation on stability of block ramps on failure mechanism of base and reinforced block ramps having different configurations such as random, row and arc disposition. They analyzed the stability of block ramps in terms of critical particle densimetric Froude number F_D and evaluated the bed evolution of the rock chute up to its failure.

They defined three stages of failure based on their observation. They are as follows:

- Initial movement: Initial movement of the base material in which base material just starts to vibrate and transportation of some elements towards downstream occurs.
- Local failure: In this one or more than one base material starts to move from the original position and producing well defined circular or semicircular scour hole.
- Global failure: The global failure of the ramp in which many local failures occur. Many boulders and part of the layers of base material gets removed. Longitudinal scour holes get formed especially in the downstream part of the ramp.

They combined experimental results with Equation (7) (flow resistance estimation for block ramp with protruding boulders) and definition of densimetric Froude number, obtained following relation for critical particle densimetric Froude number as,

$$F_{dc} = 1.98S^{0.18} \left(\frac{h}{D_{84}} \right)^{0.36} (1 + \Gamma)^{a_1} \quad (31)$$

where a_1 depends on blocks disposition: $a_1 = -2.2$ for rows, $a_1 = -2.0$ for random, $a_1 = -2.6$ for arc and $a_1 = -2.6$ and -2.8 for two different reinforced arc types configurations.

The dependency of Equation (30) on water depth h makes it difficult to use. So they further modified Equation (30) to find out critical specific discharge q_{cr}

$$q_{cr} = 1.8 S^{(-0.52+b_1)} D_{50}^{1.5} (1 + \Gamma)^{b_2} \quad (32)$$

where q_{cr} is in m^2/s and D_{50} in m.

The coefficients b_1 and b_2 depends on block disposition: $b_1 = -0.2$ and $b_2 = 1.7$ for rows, $b_1 = -0.17$ and $b_2 = 1.2$ for arc, $b_1 = -0.27$ and $b_2 = 0.8$ for random, and $b_1 = -0.17$ or -0.3 and $b_2 = 1.2$ or 0.4 for the two different reinforced arc types.

According to Raudkivi & Ettema (1982), the bimodal mixture of sediment on unstructured block ramp (UBR) consisting of random disposition of boulder of diameter D laid on bed material of characteristic diameter d_{xx} , fails in two ways. (1) Overpassing of boulders and (2) Embedding of the boulders in to finer base. According to them the dimensionless parameter consisting of two mean diameters as

D/d_{xx} controls the stability. To avoid the above failure mechanism, they had given range of value for D/d_{xx} as $6 < D/d_{xx} < 17$. Generally in mountain river, characteristics size of river bed material is taken as $d_{xx} = d_{90}$ (Janisch et al. 2007). For value of $D/d_{90} < 6$ boulder tends to move over base material and for value $D/d_{90} > 17$ boulder tends to sink in to base material causing to reduce dissipative properties of boulder. The equation suggested by Pagliara & Chivaccini (2007) for estimation of critical densimetric Froude number and critical specific discharge does not considers the effect of D/d_{xx} .

Later on, the effect of D/d_{90} was considered by Weitbrecht et al. (2017) for UBR. They carried out an experimental study on UBR consisting of protruding boulders of concentration Γ laid on a base material of characteristic diameter d_{90} . The parameters were bimodal mixture ratio D/d_{90} , block diameter D , block concentration Γ and specific discharge q . The range of parameters for study (Requena 2008) was $4.9 < D/d_{90} < 18.6$; $0.15 < \Gamma < 0.25$. Finally, the optimal range was $6.5 < D/d_{90} < 7.4$ for no ramp, failure resulting in an equilibrium slope $S_e = 30\% - 50\%$ and $\Gamma = 0.15$.

They suggested a relationship for developed equilibrium slope after a long run for design purposes based on the result of extensive experimentation as:

$$S_e = \frac{11}{200 + q_{d^*}}, \quad \text{for } q_{d^*} < 1700, \quad (33)$$

where q_{d^*} = dimensionless specific discharge. They also parametrized dimensionless specific discharge with D/d_{90} , Γ , D , and q , which is given as:

$$q_{d^*} = q / \sqrt{g(G-1)D^3} \Gamma^{-1} (D/d_{90})^2 \quad (34)$$

Using the above equation and from further literature review, block diameter D and required block concentration can be determined. Note, all the mentioned approaches do not take into account the stabilizing and destabilizing effect of incoming bed load except for the equation proposed by Weitbrecht et al. (2017). In their experiment, sediment supply as bed load showed a stabilizing effect.

Generally, we choose a straight reach of streams for a block ramp, but sometimes it becomes necessary to provide a block ramp in curved portions of streams, In that case, the

above discussed equations do not give the stable parameters of the block ramp.

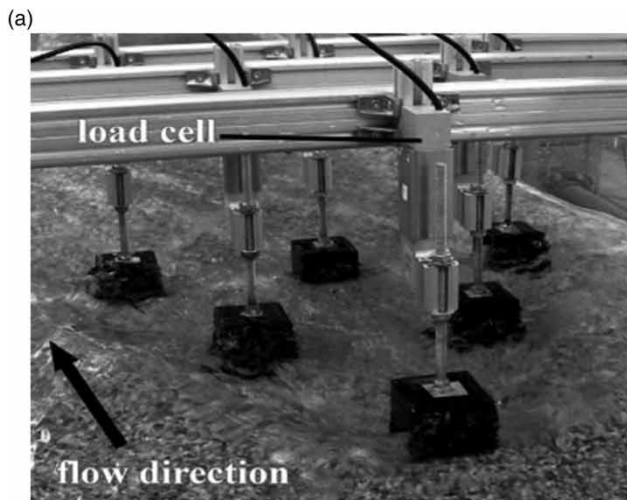
DRAG COEFFICIENT OF BOULDER ON BLOCK RAMP

In steep mountain rivers with large scale roughness, flow resistance is dominated by form drag. Drag force is a significant hydrodynamic force in gravel bed streams. Drag from channel form, bed form and immobile obstacles causes flow velocity to slow down by extracting momentum from the flow. In the block ramp, resistance is offered mainly by boulder drag, resulting in an increase in flow depth and decrease in flow velocity. Estimation of drag coefficients on the block ramp is essential for drag force, mean velocity and mean flow depth calculation. Basically, hydrodynamic force consists of two components, drag and lift force.

The drag force depends on hydrodynamic pressure $P = \rho \frac{U^2}{2}$, where ρ is medium fluid density, and U is mean flow velocity. Drag force F_D acting on projected area A_p of a boulder, having a coefficient of drag C_d , is given as (Naudascher 1991):

$$F_D = C_d \rho A_p \frac{U^2}{2} \quad (35)$$

$$C_d = 2F_D / \rho A_p U^2$$



Very little research have been done on drag coefficient estimation for block ramps, where each boulder influences the drag coefficient of others; that is, the drag coefficient of a single isolated boulder is different than boulders arranged in a group of a particular pattern. Oertel et al. (2011) did experimental work on drag coefficient estimation for boulders on a block ramp due to the flow interaction process. They used 16 different configurations of cubical as well as cylindrical boulders in rows and columns such as single blocks, double blocks in a row, and a maximum of six blocks arranged in three different rows, as shown in Figure 11(a). The configuration was chosen in such a way as to experience the boulder interaction process to determine forces and drag coefficients. The authors related drag coefficient with Reynolds number. The variation of drag coefficient versus Reynolds number is shown in Figure 11(b).

For a single boulder cube, C_d shows quasilinear dependency on the Reynolds number, as shown in Figure 12 represented by Equation (36). This shows coefficient of drag C_d increases for decrease in Reynolds number.

$$C_d = -4.0 \times 10^{-6} R + 2.1 \quad (36)$$

Similarly, it follows for a single cylindrical boulder shape but having a lower drag coefficient than a cube

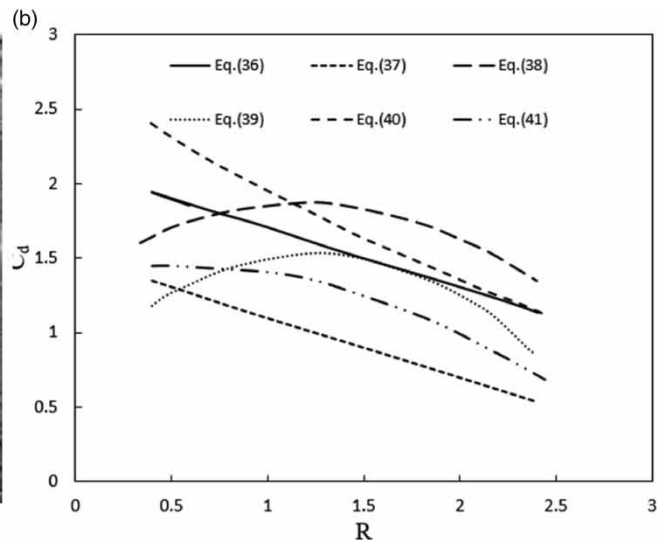


Figure 11 | (a) Photometric view of drag force measured by load cell (similar to Kothiyari et al. 2009) for cubical blocks arranged in rows and (b) coefficient of drag as a function of Reynolds number for different configurations of boulders represented by equations (Oertel et al. 2011).

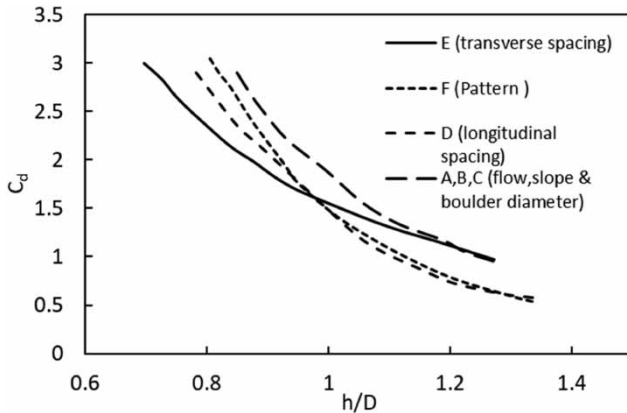


Figure 12 | Coefficient of drag as a function of submergence ratio h/D (Baki et al. 2016). Where, A,B,C,D,E and F represents series of varying parameters for flow, slope, boulder diameter, boulder longitudinal spacing, boulder transverse spacing and boulder disposition pattern respectively.

shape. In this case:

$$C_d = -4.0 \times 10^{-6} R + 1.5 \quad (37)$$

For three cubical boulders in different rows, the upstream boulder has a lower value of C_d due to the back-water effect offered by downstream boulders.

$$C_d = -3.5 \times 10^{-6} R + 1.6 \quad (38)$$

But for six boulders arranged in different rows, as shown in Figure 11(a), it shows, C_d varies in a quadratic fashion with Reynolds number.

$$C_d = -3.4 \times 10^{-11} R^2 + 8.0 \times 10^{-6} R + 1.4 \quad (39)$$

$$C_d = -4.9 \times 10^{-11} R^2 + 1.2 \times 10^{-5} R + 0.8 \quad (40)$$

Equations (39) and (40) are for downstream outer and middle boulders in the third row respectively. The variations of C_d and R , are both shown in Figure 11(b). The drag coefficient for the outer boulder of the third row is higher than the middle boulder of the same row. This is due to the fact that the upstream boulder bifurcates the main flow towards the downstream outer boulder, causing an increase in drag coefficient of the outer boulder and a decrease in drag coefficient for the middle boulder. The interaction process

decreases the drag coefficient of the upstream boulder. The interaction process becomes negligible.

When the distance between each boulder is increased, it causes a reduction in drag coefficient as represented by Equation (41):

$$C_d = 7.8 \times 10^{-12} R^2 + 8.0 \times 10^{-6} R + 2.7 \quad (41)$$

Baki et al. (2016) studied the effect of submergence on drag coefficient for various simulations of a fish pass (staggered arrangement of boulders) such as flow variation, channel slope, boulder diameter, boulder longitudinal and transverse spacing and boulder disposition pattern. They found that boulder spacing (longitudinal and transverse) and disposition pattern have a great influence on variation of drag coefficient (C_d ranged from 0.5–3.0) with submergence ratio (h/D) as depicted from Figure 12.

FURTHER RESEARCH NEEDS

A comprehensive review is presented of experimental studies relating to different configurations of block ramps covering various design aspects such as flow resistance, energy dissipation, stability and drag coefficient of the block ramp as well as its flow characteristics done by various investigators in the past. The forms and equations for estimating each of these aspects are also presented in detail. More research is warranted for further improving the equations essential for design analysis. The major grey areas and gaps that could enhance the future research are as follows.

- Three-dimensional turbulence burst analysis using a modified 3-D Reynolds stress approach using all three fluctuating instantaneous velocity components u' , v' , w' around the blocks to improve the understanding of the internal mechanism of turbulent flow structure, which is primarily responsible for energy dissipation. Present reported research on turbulent analysis is based on the 2-D Reynolds stress concept, whereas in reality turbulent burst occurrence is three dimensional. The positive end product from this research foray will significantly enhance the prediction of residual energy from block ramps much more realistically, leading to their better design.

- Even though block ramp technology is used mostly in mountainous torrents carrying highly non-uniform bed and suspended sediment loads in episodic transport mode, hardly any research is reported on this vital issue. In this respect, innovative research design is awaited for a skillful interaction between the fluvial processes of three-dimensional turbulent bursts on ejection and sweep attributes with sediment transport modes of entrainment, transport and deposition for episodic flow regimes.
- Since block ramp application in primarily hilly torrents is made in a highly turbulent flow conditions with rapidly varied unsteady flow regime, the present day formulations are based on an assumption of steady flow conditions. This steady flow assumption superimposed on 2-D Reynolds stress simplification obviously introduces probably a great deal of error with regard to actual energy loss estimation in the design of block ramps.

DATA AVAILABILITY STATEMENT

All relevant data are included in the paper or its Supplementary Information.

REFERENCES

- Aberle, J. 2000 *Untersuchung der Rauheitsstruktur zur Bestimmung des Fließwiderstandes in Gebirgsbächen Unter Klarwasserabfluss*. Mitteilung des Instituts für Wasserwirtschaft und Kulturtechnik 207, Universität Karlsruhe, D (in German).
- Aberle, J. & Smart, G. M. 2003 [The influence of roughness structure on flow resistance on steep slopes](#). *Journal of Hydraulic Research* **41** (3), 259–269.
- Abt, S. R., Whittler, R. J., Ruff, J. F. & Khattak, M. S. 1988 [Resistance to flow over riprap in steep channels](#). *Water Resources Bulletin* **24** (6), 1193–1200.
- Aguirre-Pe, J. & Fuentes, R. 1991 Movement of big particles in steep, macro-rough streams. In: *Proceedings of the 24th IAHR Congress*, Madrid, Spain, Vol. A, pp. 149–158.
- Aguirre-Pe, J., Olivero, M. L. & Mocada, A. T. 2003 [Particle densimetric Froude number for estimating sediment transport](#). *Journal of Hydraulic Engineering* **129** (6), 428–437.
- Ahmad, Z. & Srivastava, D. 2014 [Energy dissipation on block ramps with large scale roughness](#). In *5th IAHR International Symposium on Hydraulic Structures*, 25–27 June 2014, Brisbane, Australia. The University of Queensland, Brisbane, Australia.
- Ahmad, Z., Petappa, N. M. & Westrich, B. 2009 [Energy dissipation on block ramps with staggered boulders](#). *Journal of Hydraulic Engineering* **135** (6), 522–526.
- Ahmad, Z., Sharma, H. & Westrich, B. 2013 [Turbulence characteristics of flow over a block ramp](#). *Journal of Water Resource and Hydraulic Engineering* **2** (1), 21–29.
- Artur, R. P., Karol, P., Bartosz, R. P., Pitor, K. & Russel, M. 2018 [Hydrodynamic parameters in a flood impacted boulder block ramp: Krzczonówka mountain stream, Polish Carpathians](#). *Journal of Mountain Science* **15** (11), 2335–2346.
- Baiamonte, G. & Ferro, V. 1997 [The influence of roughness geometry and Shields parameter on flow resistance in gravel-bed channels](#). *Earth Surface Processes and Land Forms* **22** (8), 759–772.
- Baki, A. B. M., Zhu, D. Z. & Rajaratnam, N. 2014 [Mean flow characteristics in a rock-ramp-type fish pass](#). *Journal of Hydraulic Engineering* **140** (2), 156–168.
- Baki, A. B. M., Zhu, D. Z. & Rajaratnam, N. 2016 [Flow simulation in a rock ramp fish pass](#). *Journal of Hydraulic Engineering* **140** (2), 156–168.
- Balachandar, R. & Patel, V. C. 2002 [Rough wall boundary layer on plates in open channel](#). *Journal of Hydraulic Engineering* **128** (10), 947–951.
- Bathurst, J. C., Li, R. M. & Simons, D. B. 1981 [Resistance equation for large scale roughness](#). *J. Hydraul. Div. ASCE* **107** (12), 1593–1613.
- Bathurst, J. C. 1985 [Flow resistance estimation in mountain rivers](#). *Journal of Hydraulic Engineering* **111** (4), 625–643.
- Bezzola, G. R. 2010 *Flussbau (River Engineering)*. Vorlesungsmanuskript der Vorlesung Flussbau an der ETH Zürich, Fassung Frühjahrsemester 2010, CH [in German].
- Chanson, H. 1994 *Hydraulic Design of Stepped Cascades, Channels, Weirs and Spillways*. Pergamon, Tarrytown, N.Y.
- Chiew, Y. M. & Parker, G. 1994 [Incipient sediment motion on non-horizontal slopes: début d'entraînement de sédiments sur des lits non horizontaux](#). *Journal of Hydraulic Research* **32** (5), 649–660.
- DWA, Deutsche Vereinigung für Wasserwirtschaft, Abwasser und Abfall e.V. 2010 *fischpassierbare Bauwerke – Gestaltung, Bemessung, Qualitätssicherung*. Entwurf. Merkblatt DWA M 509, DWA, Hennef, D (in German).
- Einstein, H. A. & Banks, R. 1950 [Fluid resistance of composite roughness](#). *Transactions American Geophysical Union* **31** (4), 603–610.
- Ferro, V. 1999 [Friction factor for gravel-bed channel with high boulder concentration](#). *Journal of Hydraulic Engineering* **125** (7), 771–778.
- Ghare, A. D., Ingle, R. N., Porey, P. D. & Gokhale, S. S. 2010 [Block ramp design for efficient energy dissipation](#). *Journal of Energy Engineering* **136** (1), 1–5.
- Ghisalberti, M. & Nepf, H. 2006 [The structure of the shear layer in flows over rigid and flexible canopies](#). *Environmental Fluid Mechanics* **6** (3), 277–301.

- Griffiths, G. A. 1983 Flow resistance in coarse gravel bed rivers. *Journal of Hydraulic Division* **107** (7), 899–918.
- Habibzadeh, A. & Omid, M. H. 2009 **Bed load resistance in supercritical flow**. *International Journal of Sediment Research* **24** (4), 400–409.
- Hartung, F. & Scheuerlein, H. 1970 *Design of Overflow Rockfill Dams*. Dixieme Congrès des Grands Barrages, Montreal, CDN.
- Hey, R. D. 1979 Flow resistance in gravel bed rivers. *Journal of Hydraulic Division* **105** (4), 365–379.
- Janisch, T. 2007 Aufgelöste Blockrampen im Modellversuch – Untersuchungen an der VAW. In: *VAW-Mitteilung 201* (H.-E. Minor ed.). ETH Zürich, Switzerland, pp. 63–79 (in German).
- Janisch, T., Weichert, R. & Bezzola, G. R. 2007 Verhalten von aufgelöster unstrukturierter Blockrampen. *Wasser Energie Luft* **99** (2), 146–152 (in German).
- Jarret, R. D. 1984 **Hydraulics of high gradient streams**. *Journal of Hydraulic Engineering* **110** (11), 1519–1539.
- Keulegan, G. H. 1938 **Laws of turbulent flow in open channels**. *Journal of Research of the National Bureau of Standards* **21** (6), 707–741.
- Kothiyari, U. C., Hayashi, K. & Hashimoto, H. 2009 **Drag coefficient of unsubmerged rigid vegetation stems in open channel flows**. *Journal of Hydraulic Research* **47** (6), 691–699.
- Lange, D. 2007 Blockrampen – ökologische Bauwerke zur Sohlstabilisierung. In: *VAW-Mitteilung 201* (H.-E. Minor ed.). ETH, Zürich, Switzerland, pp. 5–21 [in German].
- Loughlin, E. M. O. & MacDonald, E. C. 1964 **Some roughness concentration effects on boundary resistance**. *La Houille Blanche* **7**, 773–782.
- LUBW Landesanstalt für Umwelt, Messungen und Naturschutz Baden-Württemberg 2006 *Durchgängigkeit für Tiere in Fließgewässern 2: Umgebungsgewässer und Fischpassierbare Querwerke*. Karlsruhe, D, LUBW (in German).
- Naudascher, E. 1991 *Hydrodynamic Forces. Hydraulic Structures Design Manual 3*. IAHR, Delft.
- Nikora, V., Goring, D., McEwan, I. & Griffiths, G. 2001 **Spatially averaged open channel flow over rough bed**. *Journal of Hydraulic Engineering* **127** (2), 123–133.
- Oertel, M. & Schlenkhoff, A. 2012a **Crossbar block ramps: flow regimes, energy dissipation, friction factors, and drag forces**. *Journal of Hydraulic Engineering* **138** (5), 440–448.
- Oertel, M. & Schlenkhoff, A. 2012b Scour Development in Basins of Cross-Bar Block Ramps. In *Proceedings 2nd IAHR European Conference*, Munich, Germany.
- Oertel, M., Peterseim, S. & Schlenkhoff, A. 2011 **Drag coefficients of boulders on a block ramp due to interaction processes**. *Journal of Hydraulic Research* **49** (3), 372–377.
- Pagliara, S. 2007 **Failure mechanisms of base and reinforced block ramps**. *Journal of Hydraulic Research* **45** (3), 407–420.
- Pagliara, S. 2007 **Influence of sediment gradation on scour downstream of block ramps**. *Journal of Hydraulic Engineering* **133** (11), 1241–1248.
- Pagliara, S. & Chiavaccini, P. 2006a **Energy dissipation on block ramps**. *Journal of Hydraulic Engineering* **132** (1), 41–48.
- Pagliara, S. & Chiavaccini, P. 2006b **Energy dissipation on reinforced block ramps**. *Journal of Irrigation and Drainage Engineering* **132** (3), 293–297.
- Pagliara, S. & Chiavaccini, P. 2006c **Flow resistance of rock chutes with protruding boulders**. *Journal of Hydraulic Engineering* **132** (6), 545–552.
- Pagliara, S. & Chiavaccini, P. 2007 **Failure mechanisms of base and reinforced block ramps**. *Journal of Hydraulic Research* **45** (3), 407–442.
- Pagliara, S. & Hager, W. H. 2004 Scour downstream of block ramps. In *Proceedings of 2nd Int. Conf. on Scour and Erosion, Singapore*. Chiew, Lim and Cheng, eds., Vol. 2, p. 215.
- Pagliara, S. & Palermo, M. 2006 Scour protection downstream of block ramps. In *Proceedings of International Conference on Scour and Erosion*. River flow 2006, Lisbon, Alves, Leal and Cardoso, eds., Vol. 2, 1725.
- Pagliara, S. & Palermo, M. 2011 **Block ramp failure mechanisms: critical discharge estimation**. *ICE Proceedings Water Management* **164** (WM6), 303–309.
- Pagliara, S., Das, R. & Palermo, M. 2008 **Energy dissipation on submerged block ramps**. *Journal of Irrigation and Drainage Engineering* **134** (4), 527–532.
- Pagliara, S., Palermo, M. & Lotti, I. 2009a **Sediment transport on block ramp: filling and energy recovery**. *KSCE Journal of Civil Engineering* **13** (2), 129–136.
- Pagliara, S., Roshni, T. & Carnacina, I. 2009b Aeration and velocity profile over block ramp elements. In *33rd IAHR Congress: Water Engineering for A Sustainable Environment*.
- Pagliara, S., Palermo, M. & Roy, D. 2019 **Experimental investigation of erosion processes downstream of block ramps in mild curved channels**. *Environmental Fluid Mechanics* **20**, 339–356.
- Raudkivi, A. J. & Ettema, R. 1982 Stability of armour layers in rivers. *Journal of Hydraulics Division* **108** (9), 1047–1057.
- Requena, P. 2008 Seitenerosion in kiesführenden Flüssen – Prozessverständnis und quantitative Beschreibung. *VAW-Mitteilung* 210, Minor, H.-E., ed. ETH Zürich, CH.
- Rice, C. E., Kadavy, K. C. & Robinson, K. M. 1988 **Roughness of loose rock riprap on steep slopes**. *Journal of Hydraulic Engineering* **124** (2), 179–185.
- Robinson, K. M., Rice, C. E. & Kadavy, K. C. 1995 Stability of Rock Chutes. In: *Proceedings of the ASCE Water Resources Conference*, San Antonio, TX, pp. 1481–1485.
- Romeji, N., Ahmad, Z. & Sharma, N. 2020 Adaptive uniform and non-uniform configuration of boulders on block ramps for river restoration. In *Proceedings of the 22nd IAHR-APD Congress 2020*, Sapporo, Japan.
- Rouse, H. 1965 Critical analysis of open-channel resistance. *Journal of the Hydraulic Division* **91** (4), 1–23.
- Scheuerlein, H. 1968 Der Rauhgerinneabfluss. Bericht der Versuchsanstalt für Wasserbau Nr. 14, Technische Universität München, D.
- Schlichting, H. 1936 **Experimentelle untersuchungen zum rauhigkeitsproblem**. *IngenieurArchiv* **7** (1), 1–34. (in German).

- Shields, A. 1936 Anwendung der Aehnlichkeitsmechanik und der Turbulenzforschung auf die Geschiebewegung. Mitteilungen der Pruessischen Versuchsanstalt für Wasserbau und Schiffbau, Berlin.
- Tamagni, S. 2013 *Unstructured Block Ramps*. PhD thesis, Mitteilungen 223, Versuchsanstalt für Wasserbau, Hydrologie und Glaziologie (VAW), ETH Zürich.
- Tamagni, S., Janisch, T. & Hager, W. H. 2008 Bed stabilization with unstructured block ramps: Physical model investigations. In: *River Flow 2008* (M. S. Altinakar, M. A. Kokpinar, Y. Darama, E. B. Yegen, N. Harmancioglu, eds) 1,2075.
- Tamagni, S., Weitbrecht, V. & Boes, R. M. 2014a An ecological and engineering view on unstructured block ramps. In *Proceeding of the 7th International Conference on Fluvial Hydraulics*, Lausanne, Switzerland. River flow 2014.
- Tamagni, S., Weitbrecht, V. & Boes, R. M. 2014b [Experimental study on the flow characteristics of unstructured block ramps](#). *Journal of Hydraulic Research* **52** (5), 600–613.
- Weibel, D. & Peter, A. 2013 [Effectiveness of different types of block ramp for fish upstream movement](#). *Journal of Aquatic Sciences* **75**, 251–260.
- Weichert, R. 2006 Bed morphology and stability of steep open channels. *VAW-Mitteilung* 192, Minor, H.-E., ed. ETH Zürich, CH.
- Weichert, R. 2007 Die Gutmütigkeit von Blockrampen im Überlastfall. In: *VAW-Mitteilung* 201, Minor, H.-E., ed. ETH Zürich, CH, 111–123.
- Weitbrecht, V., Tamagni, S. & Boes, R. M. 2017 [Stability of unstructured block ramps](#). *Journal of Hydraulic Engineering* **143** (4), 1–8.
- Whittaker, J. G. & Jäggi, M. 1986 Block ramps. Mitteilungen der Versuchsanstalt für Wasserbau, Hydrologie und Glaziologie, 91, ETH Zürich, Switzerland (in German).
- Whittaker, J. G., Hickman, W. E. & Corad, R. N. 1988 *River-bed Stabilization with Placed Blocks*. Report 3-88/3, Hydraulics Section, Central Laboratories Works Corporation, Lower Hutt, NZ.
- Wohl, E. E. & Ikeda, H. 1998 [The effect of roughness configuration on velocity profiles in an artificial channel](#). *Earth Surface Processes Landforms* **23**, 159–169.

First received 24 August 2020; accepted in revised form 13 November 2020. Available online 27 November 2020